CHALMERS
UNIVERSITY OF TECHNOLOGY

Enhanced Sliding Mode Wheel Slip Controller for Heavy Goods Vehicles

EB2020- IBC-012

Enhanced Sliding Mode Wheel Slip Controller for Heavy Goods Vehicles

Alireza Marzbanrad [1] , Fredrik Bruzelius [2], Bengt Jacobson[3], Edo Drenth[4]

[1]Development engineer at Haldex Brake Products AB, guest researcher at Chalmers University of Technology
Instrumentgatan 15, 507 Landskrona, Sweden (E-mail: alireza.marzbanrad@haldex.com, alimarz@chalmers.se)
[2]Associate professor at Chalmers University of Technology, Gothenburg, Sweden (Email: fredrik.bruzelius@chalmers.se)
[3]Full professor at Chalmers University of Technology, Gothenburg, Sweden (Email: bengt.jacobson@chalmers.se)
[4]Vice president of global vehicle dynamics at Haldex Brake Products AB, Landskrona, Sweden (Email: Edo.Drenth@haldex.com)

ABSTRACT: This paper introduces an improved version of a sliding mode slip controller for pneumatic brake system of heavy goods vehicles, HGVs. Using the Fast Actuating Brake Valve, FABV, allows to adopt advance control approaches for wheel-slip controllers which provide features such as fast dynamic response, stability and robustness. In this paper, the sliding mode algorithm which was developed for the speed dependent wheel slip control using the FABV hardware is analysed and improved. The asymptotic convergence properties of the control algorithm are proven using Lyapunov stability theory and the robustness of the method is investigated.

KEY WORDS: wheel slip control, sliding mode control, anti-lock braking

1. Introduction

The development of brake systems can be traced back to the 19th and has been continued up till today, while it is difficult to point at the first brake system inventor. In this regard, there have been advancements in brake hardware as well as the new control methods which have been developed for brake system software to be used in different vehicle functions. The most important development priority of the new brake systems is safety.

A heavy goods vehicle (HGV), is the term which is used for any truck with a gross combination mass of over 3.5 tonnes. Traditionally HGVs have significantly longer stopping distance than passenger cars. Also, they are prone to jackknife and rollover which contribute to their high share in accidents [1].

From the hardware side, as an important change, switching from mechanical drum brakes to disk brakes can be addressed. In this field there have been advancements in brake valves over the past decades. The Fast Acting Brake Valve, FABV, is a future product of Haldex with very low time constant [1] , which leads to shorter stopping distance and the potential to improve other functions of HGV.

The earliest anti-lock braking functions were developed for aircraft as early as in the 1920s. Some decades later they also entered the automotive industry. Anti-lock braking is used in both passenger cars and HGVs to prevent wheel locking. It helps to maintain directional stability and thereby mitigates risks of rollover and jack-knife in articulated vehicles.

A technology shift in brake systems has occurred in the 90s in the truck market, and an Electronic Brake System (EBS) replaced the former Anti-Lock Brake System (ABS). There are several other safety functions in which brakes are utilized together with the intelligent powertrain to be implemented on different wheels, e.g. stability control and traction control. The EBS integrates many of these safety functions, so it optimizes braking operation for different scenarios.

Wheel slip control is employed at the wheel end level to regulate the slip around the demands which are generated from a higher level in the system architecture. McLoughlin analyzed the improvement of the anti-lock brake when wheel slip control is used [2].

Different control algorithms have been adopted for the wheel slip control. Gain scheduling slip control is used for passenger cars in [3]. Using fuzzy logic in the wheel slip control design has been popular among researchers. However, this strategy doesn't come with a stability guarantee. In [4] fuzzy logic is used in the slip controller for anti-lock braking. In [5] a hybrid neuro-fuzzy approach has been proposed to keep the longitudinal wheel slip within the range of demand during braking. The ABS control strategy is updated on-line to keep the level of disk/pad wear low and increase the service time of the ABS by using the fuzzy controller in [6]. References [7] and [8] are examples of using the optimization-based control method for wheel slip. Model predictive control was developed in [9] and [10] for the wheel slip control.

Sliding-mode controller is well-known to be a powerful approach for tracking problems while being robust with respect to unknown perturbations and guarantees the convergence to the desired reference in a finite time. The controllers which are developed based on this method have been applied to many real-world problems, like aerospace control, electric power systems, electromechanical systems, and robotics [11].

Generally, the slip demand is not necessarily the peak slip but in some schemes, the peak seeking algorithm is considered as a part of the wheel slip controller. References [12] and [13] are about designing sliding mode extremum seeking algorithm, theoretical presentation and proof of stability; and in [14], [15], the application of the wheel slip control is considered. The work presented in [16] is another example, where the second-order sliding mode controller

is used for the design of the slip controller to control the traction force and also sliding mode observer to help online tire-road force estimation. In [17], three methods for the wheel slip control is investigated, PI, sliding mode PI (SMPI) and integral sliding mode. The performance of the controllers on low- and high friction surfaces have been analyzed. Also, a peak seeking algorithm has been provided to find the maximum brake force from the road-tire interaction.

The Cambridge Vehicle Dynamics Consortium, CVDC, has done extensive research on vehicle dynamics and control of HGVs. Significant improvement of longitudinal HGVs tire force control, stopping distance, maneuverability in emergency situations, is reported in [18-21]. The improvement attributes to the utilization of prototypes of fast brake actuators which made it possible to apply advanced nonlinear control methods in the brake software.

The sliding mode controller is used in the wheel slip controller which has been developed in [18]. In [1] HiL simulations has been carried out where pressure controller, a quarter car vehicle model, vehicle velocity estimator, peak seeker and force observer are the other components of the loop. Results of the simulations show oscillations of increasing amplitude in wheel slip and brake pressure. [21] applied time-varying gains, k and ϕ, of the sliding mode controller to address the issue. Simulation results show the improvement of controller performance.

The present study provides the analysis for the time-varying gain modification of [21] with some suggestions for further improvement of the algorithm. A similar quarter car vehicle model to [1] is used here. The results of the SiL is reported where the quarter car vehicle model and a slip controller are the components of the loop. Using an extremum seeking algorithm for the peak slip is not in the scope of this study. The vehicle model and the corresponding parameters are presented in Section 2. Section 3 presents the development of the sliding mode controller for the wheel slip control and development of the robustifying term to improve the performance of the controller. The results of the simulations are demonstrated in Section 4. The final comments and conclusions are presented in the final chapter.

2. Vehicle model

The planar motion of a quarter car which is moving at an uneven road surface is modeled. The model is taken from [1] which has 2 DOF vertical dynamics regarding unsprung and sprung mass and the other 2 DOF is corresponding to longitudinal motion of the vehicle and rotational motion of the wheel. The model is demonstrated in Figure 1. The motivation for modeling the vertical dynamics is to assess the robustness of the controller with respect to the road unevenness.

2.1. Longitudinal motion:

The longitudinal equation of motion is

$$F_x = m_v \dot{v}_x \qquad (1)$$

where, $m_v = m_s + m_u$ is the total mass of the vehicle and F_x is the longitudinal tire force which is derived from the UMTRI tire model. For the sake of simplicity, the aerodynamic and slope resistance forces are not considered in the model.

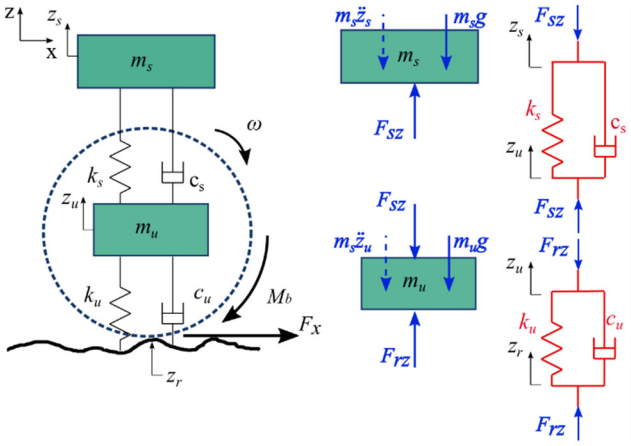

Figure 1. Quarter car vehicle model

Wheel rotation:

$$J\dot{\omega} = -r_b F_x + M_b \qquad (2)$$

where, J is the rotational moment of inertia of the wheel, ω is the wheel rotational speed, M_b is the braking torque and r_b is the radius at which braking force acts.

2.2. UMTRI tire model

This model has been developed at the University of Michigan Transportation Research Institute (UMTRI). Here, the model is presented in ISO 8855 coordinate system. The wheel slip σ_x, is:

$$\sigma_x = \frac{\omega r_r - v_x}{v_x} \qquad (3)$$

where, r_r is the rolling radius of the wheel. The braking force represented by the model is:

$$F_x = \frac{(\mu F_z)^2(1+\sigma_x)}{4C_x s_x} - \mu F_z(1+L_x) \qquad (4)$$

where, F_z is the vertical load, C_x is the longitudinal stiffness, L_x is the fraction of the contact patch which is not sliding and μ is the friction coefficient which is speed dependent in the UMTRI model according to the following equation:

$$\mu = \mu_f + (\mu_s - \mu_f)e^{\frac{(\omega r_r - v_x)}{V_f}} \qquad (5)$$

where, μ_s, μ_f are stick friction, sliding friction and V_f determines the shape of the friction function. The tire stiffness, C_x in *(4)* is dependent on normal load

$$C_x = C_1 F_z - \frac{F_z^{\,2}}{C_2} \qquad (6)$$

where, $C_1 = 10$ and $C_2 = 13345$ N. Also, L_x is calculated as

$$L_x = \frac{\mu F_z(1+\sigma_x)}{2C_x\sigma_x} \qquad (7)$$

It has a maximum value of 1. When $L_x = 1$, no sliding occurs and the shear force can be calculated by taking the integral of longitudinal deflection, and *(4)* can be rewritten as

$$F_x = \frac{C_x\sigma_x}{(1+\sigma_x)} \qquad (8)$$

2.3. Vertical dynamics

The corresponding vertical dynamics of the model which is presented in Figure 1 is

$$\begin{aligned} m_s\ddot{z}_s &= F_{sz} - m_s g \\ m_u\ddot{z}_u &= F_{rz} - F_{sz} - m_u g \end{aligned} \tag{9}$$

where F_{sz} and F_{rz} are given by:

$$\begin{aligned} F_{sz} &= k_s(z_u - z_s) + c_s(\dot{z}_u - \dot{z}_s) + m_s g \\ F_{rz} &= k_u(z_r - z_u) + c_u(\dot{z}_r - \dot{z}_u) + (m_s + m_u)g \end{aligned} \tag{10}$$

By defining $z_r = z_r(x(t))$, the excitation of the vertical dynamics can be prescribed. Vehicle simulation parameters are presented in Table 1.

Table 1. Quarter car parameters

Parameter	Symbol	Unit	Value
Wheel polar moment of inertia	J	kgm^2	13
Sprung mass	m_s	kg	1600
Unsprung mass	m_u	kg	400
Rolling radius	r_r	m	0.52
Suspension spring stiffness	k_s	kN/m	500
Suspension damping stiffness	c_s	kNs/m	15
Tire spring stiffness	k_u	kN/m	1400
Tire damping stiffness	c_u	kNs/m	2

3. Control

Let σ_{d_x} be a slip limit which is generated by a vehicle level control. The sliding surface is defined as

$$s = \sigma_x - \sigma_{d_x} \tag{11}$$

The objective is to design a controller which contributes to $s \to 0$. The time derivative of *(11)* can be written as

$$\dot{s} = \frac{\dot{\omega} r_r}{v_x} - \frac{\omega \dot{v}_x r_r}{{v_x}^2} - \dot{\sigma}_{d_x} \tag{12}$$

Using *(2)*, equation *(12)* can be rewritten as

$$\dot{s} = \frac{(-r_b F_x + M_b) r_r}{J v_x} - \frac{\omega \dot{v}_x r_r}{{v_x}^2} - \dot{\sigma}_{d_x} \tag{13}$$

So, the following control law can satisfy the control objective

$$M_b = r_b F_x + \frac{J v_x}{r_r}\left(\frac{\omega \dot{v}_x r_r}{{v_x}^2} + \dot{\sigma}_{d_x}\right) - k\, sgn(s) \tag{14}$$

where, $sgn(.)$ is the sign function and k is the sliding gain. Substituting *(14)* in *(13)* results in

$$\dot{s} = -\frac{k\, r_r\, sgn(s)}{J v_x} \tag{15}$$

For the purpose of chattering attenuation, the sign function can be replaced by a sigmoid function. The proportional term is added to reduce the rise time of convergence. Substituting sign function with these terms yields

$$M_b = r_b F_x + \frac{J v_x}{r_r}\left(\frac{\omega \dot{v}_x r_r}{{v_x}^2} + \dot{\sigma}_{d_x}\right) - \left(k\frac{s}{|s| + \delta} + \phi s\right) \tag{16}$$

$$\dot{s} = -\frac{r_r}{J v_x}\left(k\frac{s}{|s| + \delta} + \phi s\right) \tag{17}$$

where, δ is used to define a boundary layer to reduce the chattering and ϕ is the positive constant. For the sliding surface dynamics, the following positive definite function is a Lyapunov candidate

$$V = \frac{1}{2}s^2 \tag{18}$$

The time derivative of *(18)* is

$$\dot{V} = s\dot{s} = = -\frac{r_r}{J v_x}\left(k\frac{s^2}{|s| + \delta} + \phi s^2\right) \leq 0 \tag{19}$$

which shows the asymptotic stability of sliding surface dynamics with the designed control law. The control law*(16)*, is reported by CVDC in [18]. [21] reported the deficiency of the controller that leads to the oscillations with the increasing amplitude at low speed which increases air consumption. In order to address the chattering, [21] suggests modifying the sliding mode gain k to vary with velocity linearly. The sliding gain k and the proportional gain ϕ are multiplied by the following scaling factor:

$$k = a v_x + b \tag{20}$$

where, a and b are slope and the offset of the scaling factor which is set to 20% of the initial speed of braking. Test results show a substantial reduction in air consumption at low speeds with this modification. Nevertheless, the analysis of the modifications has not been provided. In *(17)*, the dynamics of the sliding surface is dependent on the inverse of the vehicle speed. As a result, at low speeds the dynamics tend to infinity which generates the undesired chattering. It should be noted that even with the modification *(19)* the problem persists. To illustrate, let's replace k in *(16)* with *(20)* and without loss of generality let $\phi = 0$, sliding surface dynamics in *(17)* will be

$$\dot{s} = -\frac{r_r(a v_x + b)}{J v_x}\left(\frac{s}{|s| + \delta}\right) = -\left(\frac{r_r a}{J} + \frac{r_r b}{J v_x}\right)\left(\frac{s}{|s| + \delta}\right) \tag{21}$$

Here, the term $\frac{r_r b}{J v_x}$, leads the sliding surface to tend to infinity. Although, the modification improves the performance because at low speeds the parameter $k \to b$. Therefore, it is smaller than k at the beginning of braking. The problem of oscillations with increasing amplitude can also be addressed by using the time-varying gains in *(16)* as follows

$$k' = \frac{J v_x}{r_r} k, \quad \phi' = \frac{J v_x}{r_r}\phi \tag{22}$$

Using *(22)*, the control law *(16)* and the sliding surface dynamics will be

$$M_b = r_b F_x + \frac{J v_x}{r_r}\left(\frac{\omega \dot{v}_x r_r}{{v_x}^2} + \dot{\sigma}_{d_x} - k\frac{s}{|s| + \delta} - \phi s\right) \tag{23}$$

$$\dot{s} = -\left(k\frac{s}{|s| + \delta} + \phi s\right) \tag{24}$$

As it is shown in *(24)*, the sliding surface dynamics is not explicitly speed-dependent anymore. The reason [21] proposed to use the offset b is to avoid using very small values of k and ϕ at low speed. If the sliding surface has not been reached, there is a risk that the weak feedback is not actuated leading to a steady-state error or the loss of stability due to disturbances. However, for very low speeds, other issues become prominent, such as speed encoder resolutions, and these situations need to be dealt with separately. It is difficult to provide the holistic method to tune the parameter for different braking scenarios when the offset b is used to address the error.

Here, the analytical development of a robust term to address the problem is presented. Prior to bringing up a solution, it should be noted that it is mainly uncertainties and disturbances which are needed to cope with; otherwise, the convergence would not occur. These terms are invisible in equation *(19)*. The reason that k should not be less than a certain offset is to overcome the uncertainties and satisfy $\dot{V} \leq 0$. To elaborate more, consider the estimated variables in the control law, F_x and v_x. Estimation error could crash the slip control loop stability if it is not robust enough.

Let's assume that the implemented brake torque, $\widehat{M}_b$ which deviates from the ideal brake torque, M_b in *(23)*, due to force and reference velocity estimations' error is defined as

$$M_b = \widehat{M}_b + \epsilon_M \quad \text{where} \quad |\epsilon_M| < \bar{\epsilon}_M \qquad (25)$$

and the $\bar{\epsilon}_M$ is the maximum deviation from the ideal brake torque. Using the $\widehat{M}_b$in *(13)* gives

$$\dot{s} = \frac{(-r_b F_x + M_b - \epsilon_M) r_r}{J v_x} - \frac{\omega \dot{v}_x r_r}{{v_x}^2} - \dot{\sigma}_{d_x}$$

$$\dot{s} = -\left(k \frac{s}{|s| + \delta} + \phi s\right) - \frac{\epsilon_M r_r}{J v_x} \qquad (26)$$

Then the derivative of Lyapunov function *(18)* will be

$$s\dot{s} = -\left(k \frac{s^2}{|s| + \delta} + \phi s^2\right) - \frac{\epsilon_M r_r s}{J v_x} \leq -\left(k \frac{s^2}{|s| + \delta} + \phi s^2\right) + \frac{\bar{\epsilon}_M r_r}{J v_x} |s| \qquad (27)$$

From *(27)*, it is more clear that the estimation errors may violate the negative sign of Lyapunov time derivative and consequently the asymptotic convergence to the slip limit. In order to compensate the uncertainties, the robust term, M_r, is introduced:

$$M_r = -\frac{s|s|\bar{\epsilon}_M}{\mu_0 s^2 + \mu_1} \qquad (28)$$

with $0 < \mu_0 \leq 1$. $\mu_1 > 0$ is the time-varying design parameter.

The update law for μ_1 is designed according to

$$\dot{\mu}_1 = -\frac{\gamma r_r}{J v_x} \frac{|s|\bar{\epsilon}_M}{\mu_0 s^2 + \mu_1} \qquad (29)$$

where, γ is a positive constant. Adding M_r to the control law in *(23)*, the $\dot{s}$ will be derived as:

$$\dot{s} = -\left(k \frac{s}{|s| + \delta} + \phi s\right) - \frac{\epsilon_M r_r}{J v_x} - \frac{s|s|(\bar{\epsilon}_M r_r)}{J v_x (\mu_0 s^2 + \mu_1)} \qquad (30)$$

The Lyapunov candidate to investigate the stability of the new system is $V = \frac{s^2}{2} + \frac{{\mu_1}^2}{2\gamma}$. The time derivate of the function is

$$\dot{V} = -\left(k \frac{s^2}{|s| + \delta} + \phi s^2\right) - \frac{\epsilon_M r_r s}{J v_x} - \frac{s^2|s|(\bar{\epsilon}_M r_r)}{J v_x (\mu_0 s^2 + \mu_1)} - \frac{\mu_1 |s|(\bar{\epsilon}_M r_r)}{J v_x (\mu_0 s^2 + \mu_1)}$$

$$\dot{V} \leq -\left(k \frac{s^2}{|s| + \delta} + \phi s^2\right) - \frac{\bar{\epsilon}_M r_r}{J v_x (\mu_0 s^2 + \mu_1)} (-\mu_0 s^3 - \mu_1 s + s^2|s| + \mu_1 |s|)$$

$$\dot{V} \leq -(.) - \frac{\bar{\epsilon}_M r_r}{J v_x (\mu_0 s^2 + \mu_1)} \left(s^2(|s| - \mu_0 s) + \mu_1(|s| - s)\right) \leq 0 \qquad (31)$$

4. Simulation results

The simulation setup consists of a quarter car vehicle model and a slip controller. Other components such as the pressure controller and force observer are not included. The extremum seeking algorithm is not employed here and the constant slip limit is prescribed in the simulations. The condition is a steady-state speed of 90 km/h with zero slip on high friction smooth road. After one second driver applies a brake ramp of 20000 Nm/s. The slip limit is set to 0.2, which is slightly higher than the slip at peak force. Two scenarios are simulated. The first one is the ideal case with no other uncertainties. In the second scenario, a disturbance signal with an amplitude in a range of (-3000, 3000) N is applied to the longitudinal road-tire force during braking. For each scenario, the simulations are carried out with 4 different controllers that are denoted with (a) to (d) according to

Ref. [18]	Ref. [21]	eq. *(23)*	eq. *(23)*+*(28)*
(a)	(b)	(c)	(d)

In the second scenario, the same disturbance signal is applied to all simulated controllers. Controller parameters for each control law is presented in Table 2. For the controller with the robustifying term, (d), $\gamma = 25$ and $\mu_1(t_0) = 1$ was used. In the plots, slips and torques are shown with a positive sign to be comparable with the other works not using ISO 8855 coordinate system.

Table 2. Controllers parameters for both simulation scenarios

Controller	k	δ	ϕ	a	b	$\bar{\epsilon}_M$	μ_0
a	6	0.02	10	0	246.2	0	0
b	2	0.02	20	$25v_x$	$5v_0$	0	0
c	6	0.02	5	$25v_x$	0	0	0
d	2	0.02	8	$25v_x$	0	2000	1

Scenario 1:

According to chapter 4, the controller (a) contributes to oscillations of increasing amplitude at low speed which can be seen in Figures 3(a), 4(a). Using controller (b), oscillations at low speed are decreased, c.f. Figure 3(b), together with the switching brake torque which converges to a constant value, see Figure 4(b). The amplitude of oscillation and the switching brake torque converges to zero when the controller (c) is applied, Figure 3(c), 4(c). Employing the robust term provides a faster convergence to the slip limit at low speed, see Figure 3(d).

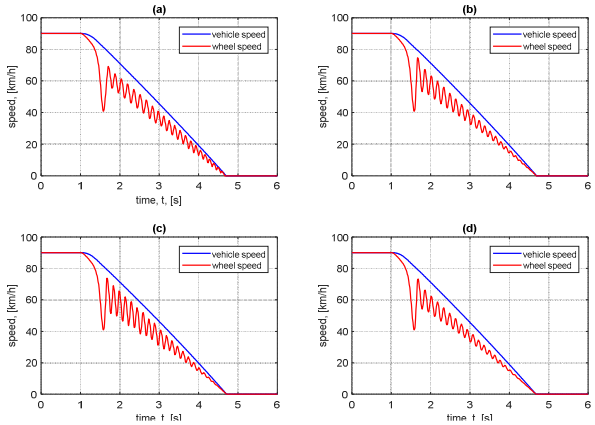

Figure 2. Speed profiles- controllers (a) to (d), scenario 1

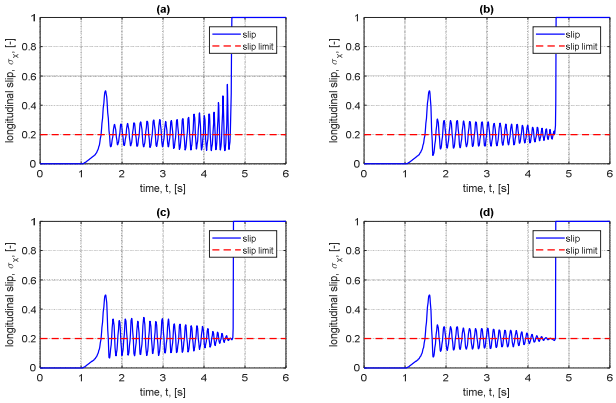

Figure 3. Slip and slip limit- controllers (a) to (d), scenario 1

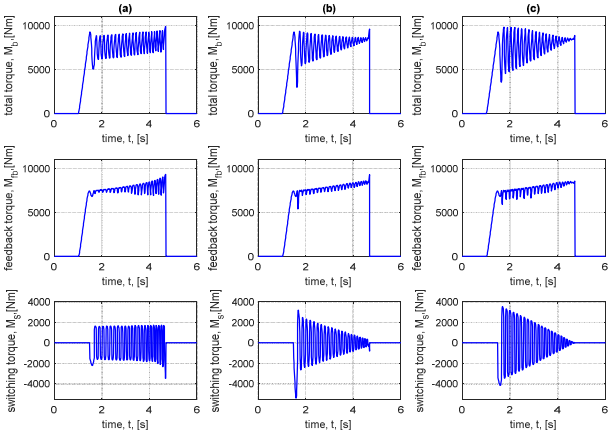

Figure 4. Total brake torques and its components controllers (a) to (c), scenario 1

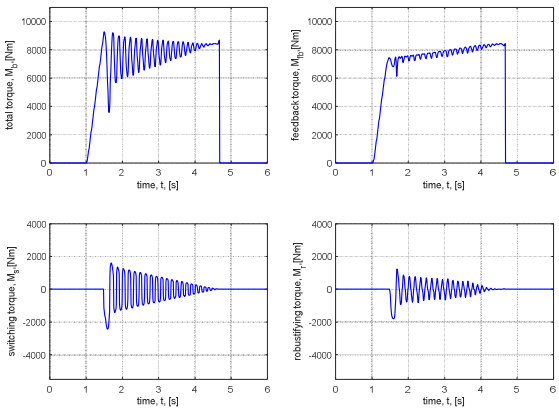

Figure 5. Total, feedback, switching and robust torques from controller (d)-scenario 1

Scenario 2:

The disturbance signal which is applied on F_x is shown in Figure 6.

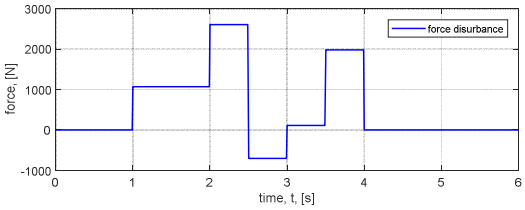

Figure 6. External disturbance signal applied in scenario 2

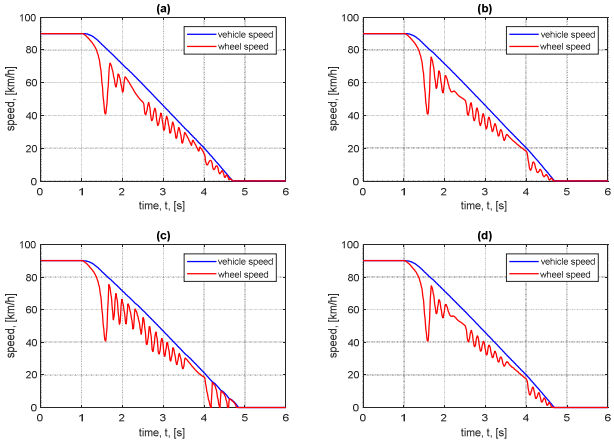

Figure 7. Speed profiles- controllers (a) to (d), scenario 2

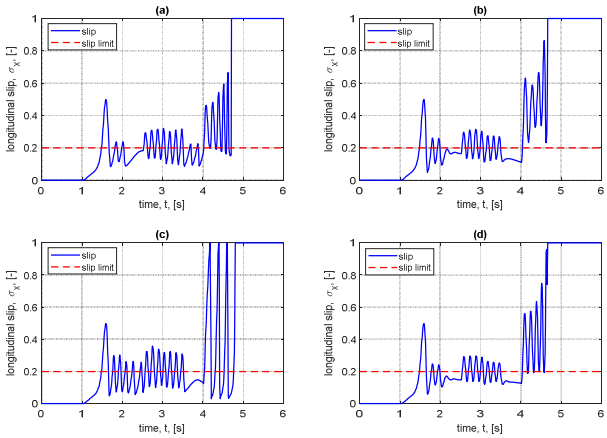

Figure 8. Slip and slip limit- controllers (a) to (d), scenario 2

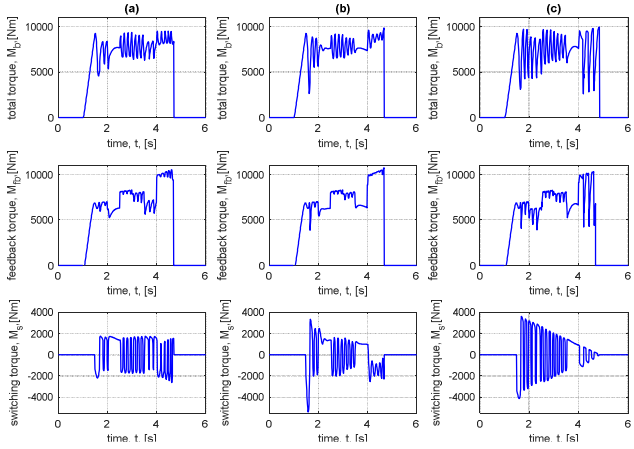

Figure 9. Total brake torques and its components controllers (a) to (c), scenario 2

As it is shown in Figure 8(a), the controller (a) is robust enough to cope with the disturbances and manages to regulate the slip around

the slip limit. Using the scaling factor in (b), gives the results in Figure 7(b), 8(b). These figures illustrate that a decrease of scaling gain at low speeds in controller (b), increases sensitivity to disturbances and the controller does not manage to regulate the slip around the slip limit. However, wheel lock does not occurr. The problem is even worse with the controller (c) where wheel lock happens (see Figures 7(c) and 8(c)) at about 20 km/h due to the convergence of switching gains to zero.

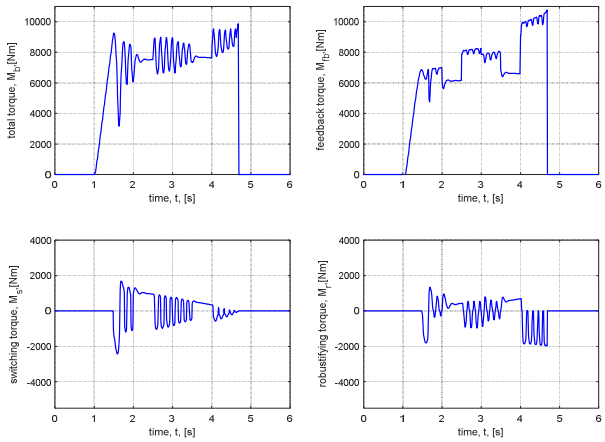

Figure 10. Total, feedback, switching and robust torques from controller (d) - scenario 2

The robust term *(28)* tackles the issue and leads to slightly better results than the controller (a), Figures 7(d), 8(d). The robust term, proposed in this paper, gives more ability and flexibility to cope with uncertainties and noises. It consumes less air while the performance of the controller is improved comparing to previous works.

5. Conclusion

This study presents a sliding mode slip controller extend previous works. The behavior of the controllers is analyzed and a robustifying term is introduced to improve the performance of the controller. Stability is shown using Lyapunov stability theory. Simulations confirm theoretical analysis. In a previously suggested controller, high air consumption occurs due to an unnecessary increase of brake torque for low speeds. It is shown that a suggested compensation for high air consumption has difficulty to cope with the disturbances at low speeds. For a presented controller with a new term, it can be shown that robustness of the controller is improved with low air consumptions. In addition, it provides more flexibility to compensate for uncertainties and disturbances in general.

References

[1] Miller J., Cebon. D., "Tyre curve estimation in slip-controlled braking" Automobile Engineering, p. 332–351, 2016.
[2] McLoughlin. J. H., "Limited Slip Braking" in Proceedings of the Symposium on Anti-Lock Braking Systems for Road Vehicles, London, 1985.
[3] Sun. J. Liu Y., "Target Slip Tracking Using Gain Scheduling for Antilock Braking Systems" in Proceedings of the American Control Conference, Washington, 1995.
[4] Akey. M., "Development of Fuzzy Logic ABS Control for Commercial Trucks" SAE Journal, pp. 780-788, 1995.
[5] Ćirović V., Aleksendrić D., "Adaptive neuro-fuzzy wheel slip control" Expert Systems with Applications, vol. 40, no. 13, pp. 5197-5209, 2013.
[6] El-Garhy A., M. El-Sheikh G. A., El-saify M. H., "Fuzzy Life-Extending Control of Anti-Lock Braking System" Ain Shams Engineering Journal, vol. 4, no. 4, pp. 735-751, 2013.
[7] Baslamisli S. C., Köse E., Anlas G., "Robust Control of Anti-Lock Brake System" Vehicle System Dynamics, vol. 45, no. 3, p. 217 – 232, 2007.
[8] Mirzaeinejad H., Mirzaei M., "A novel method for non-linear control of wheel slip in anti-lock braking systems" Control Engineering Practice, vol. 18, no. 8, pp. 918-926, 2010.
[9] Satzger C., Castro R., Knoblash A., "Robust Linear Parameter Varying Model Predictive Control and its Application to Wheel Slip Control" in IFAC-Papers OnLine, 2017.
[10] Anwar. S., "Brake-Based Vehicle Traction Control via Generalized Predictive Algorithm" in Proceedings of the 2003 SAE World Congress, Detroit, 2003.
[11] Shtessel Y., Edwards C., Fridman L., Levant A., "Sliding-mode control and observation", New York: Springer , 2014.
[12] Drakunov S., Özguner U., "Optimization of nonlinear system output via sliding mode approach" in Proceedings of the IEEE International Workshop on Variable Structure and Lyapunov Control of Uncertain Dynamical Systems, Sheffield, 1992.
[13] Pan Y., Özguner U., Acarman T., "Stability and performance improvement of extremum seeking control with sliding mode" International Journal of Control, vol. 76, no. 9-10, pp. 68-985, 2003.
[14] Drakunov S., Özguner U., Dix P., "ABS control using optimum search via sliding modes" in IEEE Transactions on Control Systems Technology, 1995.
[15] Haskara I., Özguner U., Winkleman J., "Wheel slip control for antispin acceleration via dynamic spark advance" IFAC Journal of Control Engineering Practice, vol. 8, no. 10, p. 1135–1148, 2000.
[16] Amodeo M., Ferrara A., Terzaghi R., Vecchio C., "Wheel Slip Control via Second-Order Sliding-Mode Generation" IEEE TRANSACTIONS ON INTELLIGENT TRANSPORTATION SYSTEMS, vol. 11, , pp. 122-131, 2010.
[17] Savitski D., Schleinin D., Ivanov V., Augsburg K., "Robust Continuous Wheel Slip Control With Reference Adaptation: Application to the Brake System With Decoupled Architecture," IEEE TRANSACTIONS ON INDUSTRIAL INFORMATICS, vol. 14, no. 9, pp. 4212-4223, 2018.
[18] Miller J., "Advanced braking systems for heavy vehicles", University of Cambridge, PhD Thesis, 2010.
[19] Kienhofer F., "Heavy Vehicle Wheel Sip Control, University of Cambridge", PhD Thesis, 2011.
[20] Morrison G., "Combined emergency braking and cornering of articulated heavy vehicles", Cambridge University, PhD Thesis, 2016.
[21] Henderson L., "Improving Emergency Braking Performance of articulated heavy vehicles", Cambridge University, PhD Thesis, 2013.
[22] Goodarzi. A., Alirezaei. M., "Integrated fuzzy/optimal vehicle dynamic control" International Journal of Automotive Technology, vol. 10, pp. 567-575, 2009.